JOURNAL OF CATALYSIS **103**, 270–279 (1987)

Infrared Spectroscopic Study of the Interaction of Ammonia and Oxygen at the Surface of MgO–CoO Solid Solutions

E. ESCALONA PLATERO, S. COLUCCIA, AND A. ZECCHINA

Istituto di Chimica Fisica, Università di Torino, Via P. Giuria 7, 10125 Torino, Italy

Received November 25, 1985; revised July 21, 1986

The interaction between NH_3 and O_2 at room temperature at the surface of MgO–CoO solid solutions gives oxidized products. The detailed vibrational assignment of the main infrared bands observed after the interaction demonstrates that the oxidized species are mainly constituted by NO_2^- and NO_3^- groups adsorbed on the surface.

INTRODUCTION

The catalytic oxidation of NH_3 is a chemical reaction of considerable industrial importance.

The reaction occurs on both metallic (Pt, Rh, etc.) and oxidic systems (*1–5*). On several oxides M_xO_y (Co_3O_4, MnO_2, CuO, Fe_2O_3, V_2O_5) the oxygen activation is thought to occur via the initial formation of atomic negative oxygen ions bound to oxidized forms of the cations. These negative ions then react with NH_3 to form imide NH species which are further oxidized into nitroxyl groups (*6*) and more highly oxidized species.

It is consequently of considerable mechanistic interest to investigate the reactivity of anionic oxygen species toward NH_3 adsorbed at the surface.

The interaction of NH_3 and O_2 with MgO–CoO solid solutions has been previously reported in two separate contributions (*7, 8*). The relevant results of these investigations can be summarized as follows.

Three forms of adsorbed NH_3 have been observed:

(a) a very weakly adsorbed form (peaks at 3307, 3217, ~1625, and 1015 cm^{-1});

(b) a molecular (reversible) species coordinated to Mg^{2+} and Co^{2+} ions (peaks at 3330, 3225, 1598, and 1040 cm^{-1});

(c) an irreversible species dissociated on $Mg^{2+}(Co^{2+})O^{2-}$ pairs (with formation of NH_2^- and OH^- groups).

Moreover, no appreciable difference was observed between the adsorptive capacity (toward NH_3) of pure MgO (*9*) and co-diluted MgO–CoO solid solutions (*7*).

The previous results suggest that the *MgO matrix acts as ammonia activator via both dissociative and nondissociative (coordinative) chemisorption* (*9*).

As far as oxygen adsorption on MgO and MgO–CoO solid solutions is concerned (*8*), the following can be observed. On pure MgO the oxygen adsorption is negligible. On solid solutions two types of adsorbed oxygen have been observed:

(a) a reversible (molecular) species, characterized by stretching frequencies in the range 1250–1100 cm^{-1} having superoxo Co^{3+} O_2^- structure (the observed multiplicity of these specie is due to the surface heterogeneity) (*8*);

(b) an irreversible (atomic) species, derived from dissociation of the oxygen molecules on $(Co^{2+}\ O^{2-})_n$ aggregates emerging on the surface.

A further irreversible species with O_2^- structure has also been observed by ESR by Cordischi *et al.* (*10*).

From these results it was deduced that *Co^{2+} ions at the surface of solid solutions*

0021-9517/87 $3.00

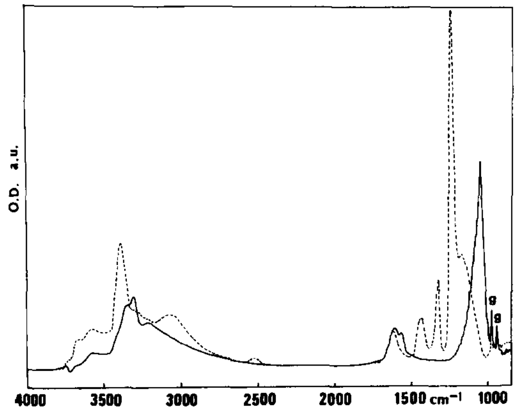

FIG. 1. IR spectrum of NH_3 adsorbed on a MgO–CoO solid solution (P_{NH_3} = 20 Torr) before (full line) and after interaction with $^{16}O_2$ (P_{O_2} = 10 Torr) (broken line). The letter g indicates the bands of the gas phase.

can act as activators of the oxygen molecule in strict analogy with homogeneous Co^{2+} complexes with similar structure (11).

As the chemisorption (activation) of NH_3 and O_2 occurs plausibly on separate sites (on the matrix and on implanted Co^{2+} ions, respectively), it is expected that their simultaneous chemisorption can occur without mutual displacement and that their chemical interaction can consequently occur via well-known adsorbed precursors.

From these considerations it is inferred that solid solutions can be used as model compounds to elucidate the interaction of NH_3 and oxygen on oxidic compounds.

In this paper the O_2–NH_3 interaction on MgO–CoO solid solutions is investigated and the structure of the surface species formed by chemical reaction in the adsorbed state has been elucidated by means of IR spectroscopy.

EXPERIMENTAL

The IR spectra were recorded with a Perkin–Elmer PE 580 B spectrometer equipped with a data station.

The MgO–CoO solid solutions containing 0.05 *M* fractions (MC 5) of CoO were prepared following standard procedures (*12*). Before dosing O_2, NH_3, and O_2/NH_3 mixtures, the samples were outgassed at 1073 K for 3 h under high vacuum.

The specific surface area (BET) of MC 5 solid solution was typically in the range 100–150 m^2 g^{-1}.

The $^{16}O_2$, $^{18}O_2$, $^{14}ND_3$, $^{14}NH_3$, and $^{15}NH_3$ gases utilized in this investigation were of high purity grade.

RESULTS

In Fig. 1 the IR spectra of NH_3 adsorbed on a MgO–CoO solid solution (P_{NH_3} = 20 Torr) before (full line) and after interaction with $^{16}O_2$ (P_{O_2} = 10 Torr) (broken line) are illustrated.

It can be seen that:

(i) the peaks at 3307, 1557, and 1015 cm^{-1} disappear;

(ii) new peaks at 3740, 3680, 3580, 3400, 3060, 1435, 1319, 1226, 1168, and 1048 cm^{-1} are formed at the expense of the previous ones, and these are due to NH_3–O_2 interaction products formed at the surface of the solid solution.

As shown in Fig. 2 (where the effect of outgassing at room temperature is illustrated) some of the new species are very strongly adsorbed (peaks at 3740, 3680, 1435, 1319, 1226, and 1048 cm^{-1}) while some others are at least partially desorbed at room temperature simply by lowering the equilibrium pressure (peaks at 3400, 1625, 1168, 968, and 933 cm^{-1}). The narrow peaks at 968 and 933 cm^{-1}, which disappear very soon upon outgassing, are due to gaseous NH_3.

From Fig. 2 it can also be seen that the removal of NH_3 from the gas phase is accompanied by the attenuation of the broad peaks at 3580 and 3060 cm^{-1} and by the contemporary increase of the narrow peak at 3740 cm^{-1}. The growth of the 3740-cm^{-1} peak could be due to the transformation of hydrogen bonded OH··NH_3 groups into free OH hydroxyls (*13*) by removal of NH_3 (*14*). In order to demonstrate that NH_3 can interact with the OH groups of the surface,

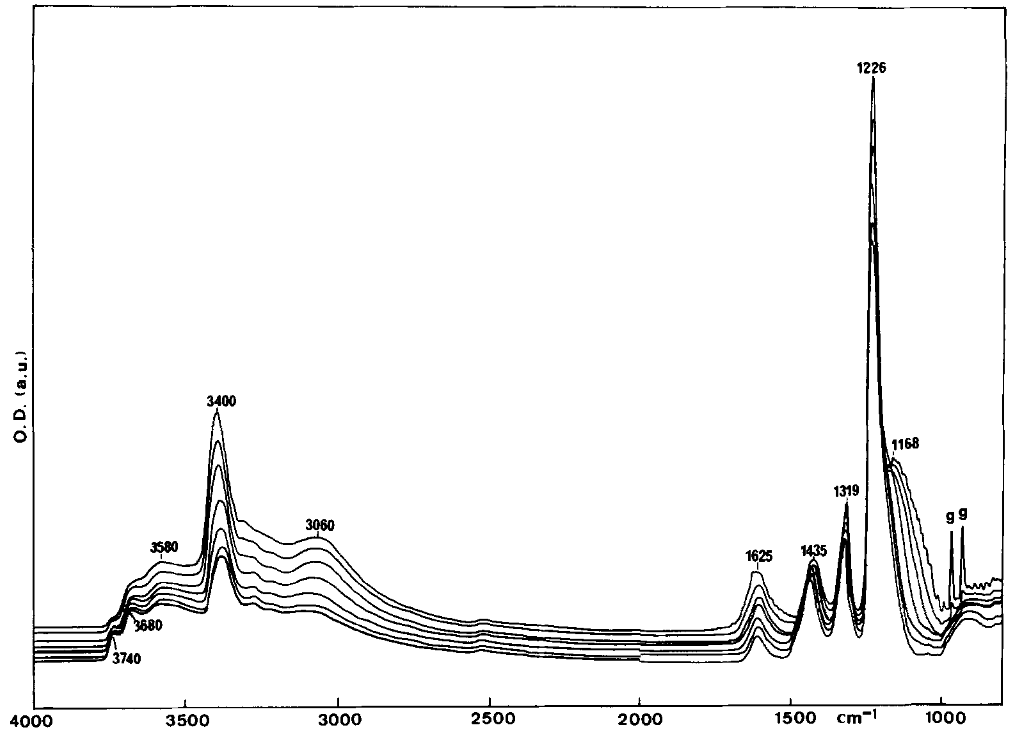

FIG. 2. Effect of outgassing at room temperature for increasing time on the IR spectrum of adsorbed NH_3–O_2 mixture. The letter g indicates the bands of the gas phase.

the spectra of NH_3 adsorbed on highly dehydrated (Fig. 3a) and on fully hydroxylated MgO matrix (Fig. 3b) have been compared (*15*). The following can be noticed:

(i) after NH_3 adsorption, two intense and broad bands are observed at ~3600 and 3060 cm^{-1} in the spectrum of the hydroxylated sample (full line), which are very weak on the highly dehydrated sample;

(ii) the desorption at room temperature (broken curve) is accompanied by a decrease of the intensity of the 3600- and 3060-cm^{-1} bands and by a strong increment of the narrow 3740-cm^{-1} peak;

(iii) the spectrum in the region 3400–3200 cm^{-1} (unperturbed NH stretching) is different in the two cases (the ν(NH) bands are definitely stronger on fully dehydroxylated samples).

In order to help in the assignment of the IR spectrum of the interaction products of NH_3 and O_2 (with special emphasis for the IR modes involving the hydrogen atoms) the spectra of the $^{14}NH_3/^{16}O_2$ and $^{14}ND_3/^{16}O_2$ interaction products are compared in Fig. 4. It can be observed immediately that the peaks at 1435, 1319, 1226, and 1048 cm^{-1} are not influenced by the H–D substitution, and hence they must be associated with surface groups which contain only nitrogen and oxygen atoms. The remaining peaks, which on the contrary are more or less shifted by deuteration, are associated with hydrogen-containing species.

In the same figure, a correlation between equivalent peaks of hydrogen- and deuterium-containing surface compounds is indicated (together with their most likely assignment: vide infra).

The frequency of the bands associated with the species not containing hydrogen is expected to be influenced by the change of the O and N masses.

In Fig. 5, the IR spectra (2000–800 cm^{-1})

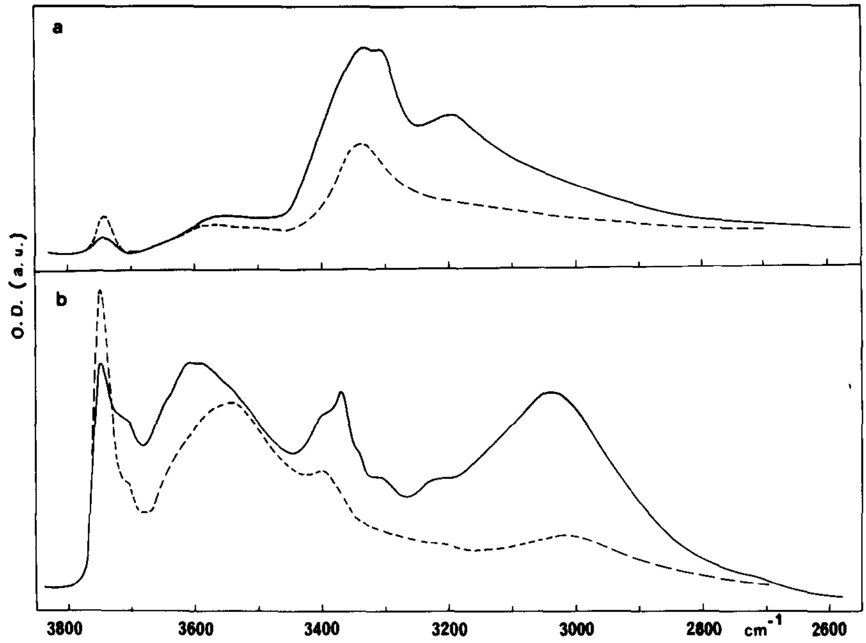

FIG. 3. (a) IR spectrum of NH_3 on MgO preoutgassed at 973 K; P_{NH_3} = 90 Torr (full line) and outgassed 1 min at room temperature (broken line). (b) IR spectrum of NH_3 on MgO preoutgassed at 473 K; P_{NH_3} = 90 Torr (full line) and outgassed 1 min at room temperature (broken line).

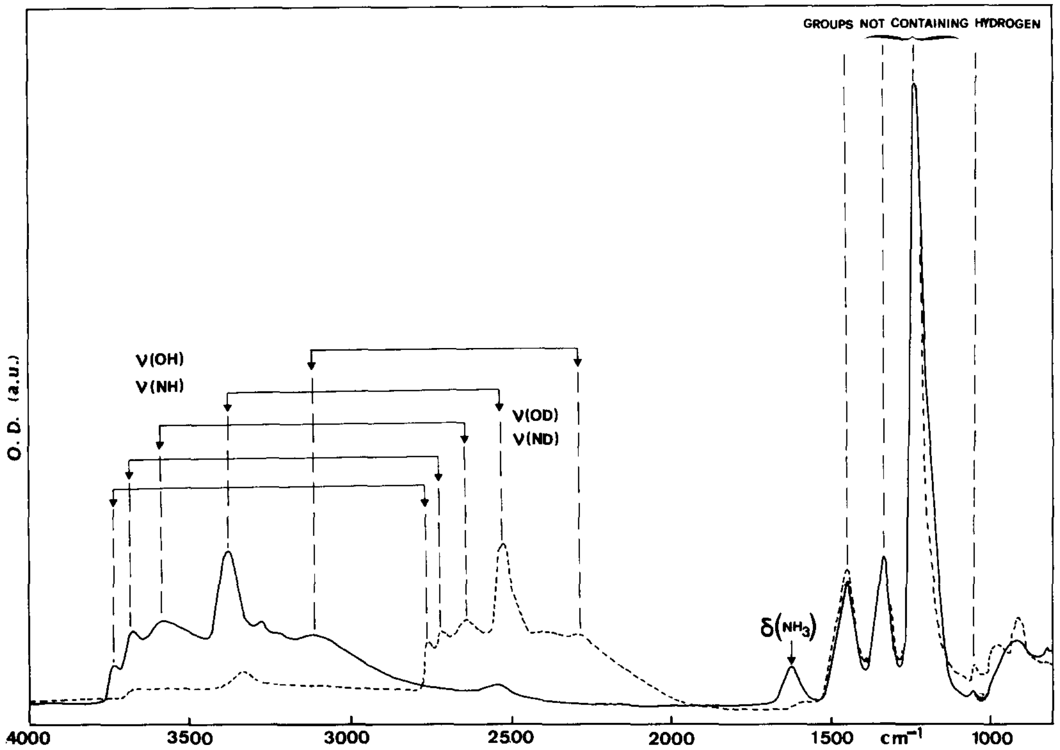

FIG. 4. IR spectra of $^{14}NH_3$–$^{16}O_2$ (full line) and $^{14}ND_3$–$^{16}O_2$ (broken line) interaction products.

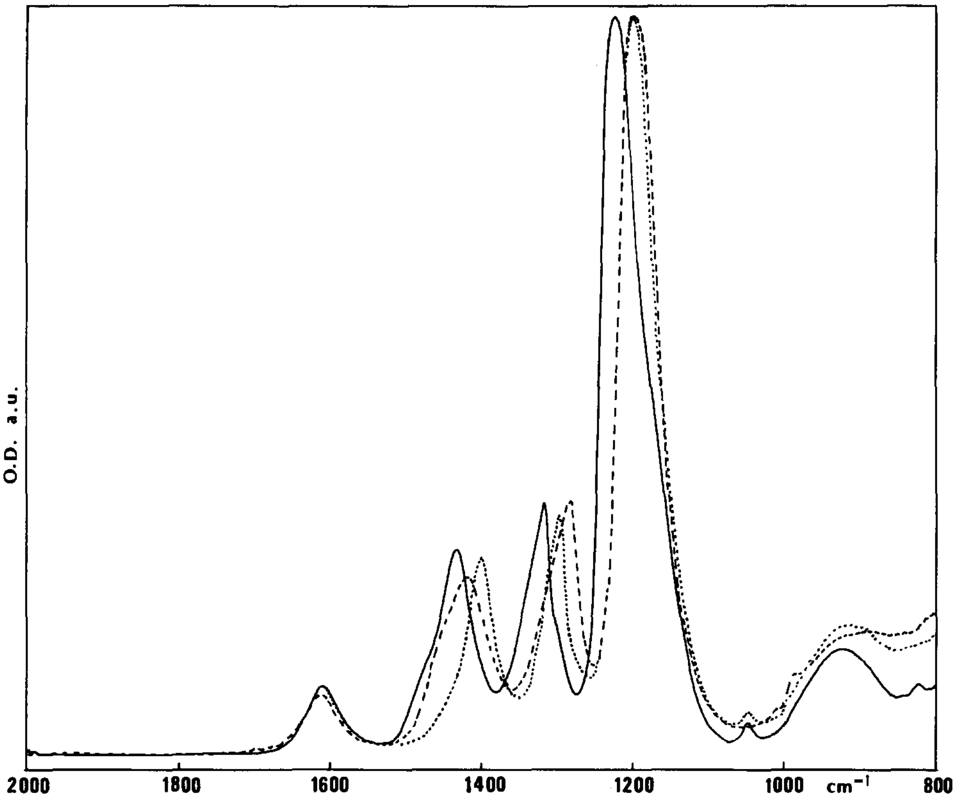

FIG. 5. IR spectra of $^{14}NH_3$–$^{16}O_2$ (full line), $^{15}NH_3$–$^{16}O_2$ (dotted line), and $^{14}NH_3$–$^{18}O_2$ (broken line) interaction products.

of the $^{16}O_2$–$^{14}NH_3$ (full line), $^{16}O_2$–$^{15}NH_3$ (dotted line), and $^{18}O_2$–$^{14}NH_3$ (broken line) interaction products are compared.

The frequency values of the four peaks associated with nitrogen- and oxygen-containing N_xO_y species are listed in the first column of Table 1.

In Fig. 6, the effect of oxygen exposure at 500 K (full line) on the species formed upon $^{15}NH_3/^{16}O_2$ interaction at room temperature (RT) is illustrated.

It can be seen that:

(i) the peak at 1204 cm^{-1} totally disappears;

(ii) three absorptions at 1430–1400, 1300–1270, and 1048 cm^{-1} grow simultaneously at the expense of the previous one.

Finally, in Fig. 7, the RT NH_3 adsorption on the fully oxidized sample is illustrated. It can be seen immediately that the separation between the two main peaks characteristic of the fully oxidized samples decreases with increase of the quantity of adsorbed NH_3. This effect is reversible: in fact, if

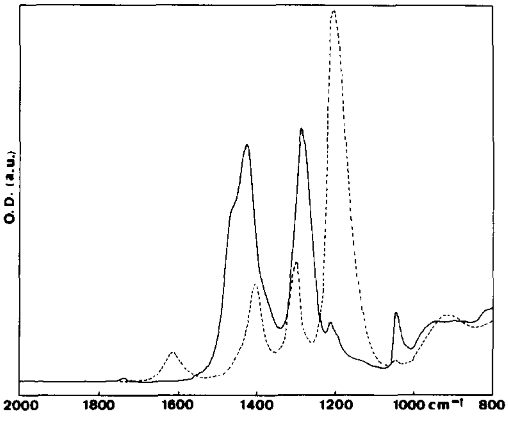

FIG. 6. Effect of oxidation at 500 K. Broken line, original spectrum ($^{15}NH_3$–$^{16}O_2$); full line, after oxygen contact at 500 K.

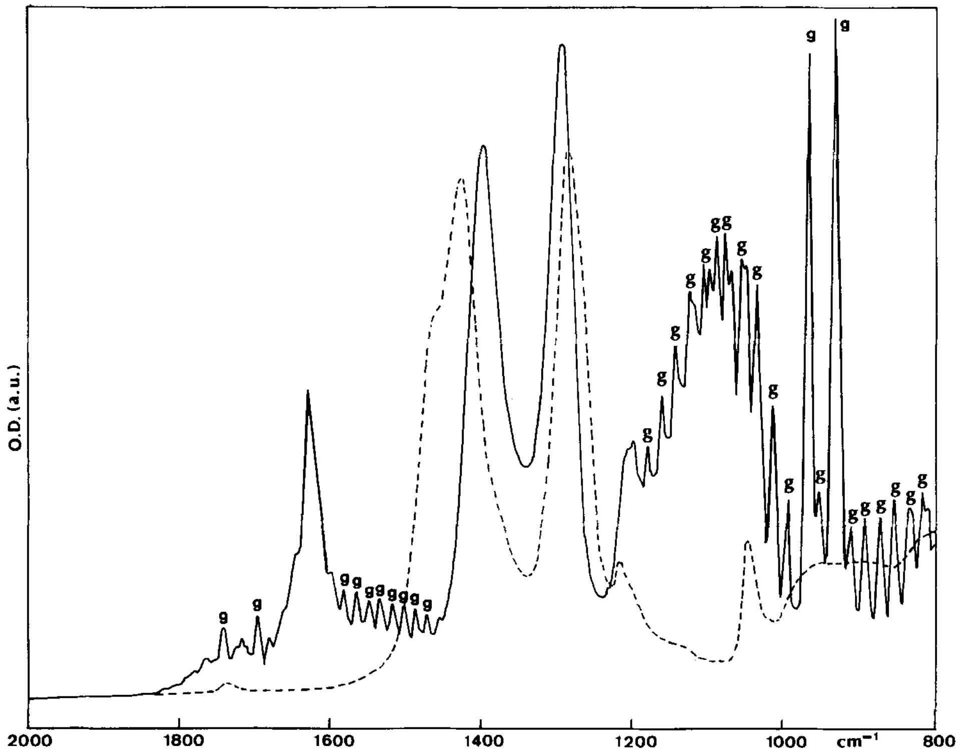

FIG. 7. IR spectrum of a fully oxidized sample before (broken line) and after NH_3 adsorption (P_{NH_3} = 200 Torr) (full line). The letter g indicates the gas-phase bands.

NH_3 is removed by reducing the gas pressure, the separation between the two peaks goes back to the original value.

DISCUSSION

The IR Spectrum of Adsorbed NH_3

The spectrum of NH_3 adsorbed on the MC 5 solid solution (Fig. 1) is very similar to that of NH_3 adsorbed on pure MgO (*9*). Both spectra have been explained in terms of the presence of at least three surface species.

One of them (species I: peaks at 3335, 3250, 1557, and 1102 cm^{-1}) is formed via a dissociative process, following the scheme:

$$Me^{2+}O^{2-} + NH_3 \rightarrow \overset{NH_2^-}{Me^{2+}}OH^- \qquad Me = \mathrm{Mg,Co}, \quad (1)$$

whereby the involved ions are in a low-coordination state and are probably located on the edges, steps, and corners of the particles. The simultaneous formation of OH^- groups is well evidenced by the peaks at 3740, 3680, 3580, and 935 cm^{-1} associated with the stretching and bending modes of the hydroxyls.

The other bands correspond to undissociated NH_3, because they are readily attenuated by lowering the gas pressure. They have been assigned to NH_3 coordinated on Me^{2+} cations (species II: peaks at 3330, 3225, 1598, and 1040 cm^{-1}) and to NH_3 in a liquid-like state (species III: 3307, 3217, 1625, and 1015 cm^{-1}).

The two shoulders at ~3405 and 3425 cm^{-1} have been left unassigned on both MgO and MgO–CoO solid solutions (*7, 9*).

In the dissociative path 1, OH^- and NH_2^- groups are formed in equal amounts.

Thus we have to consider the possibility that NH_2^- and OH^-, once formed, can act as adsorbing centers toward incoming NH_3 molecules, giving new molecular forms of adsorbed NH_3 (so explaining the presence of the shoulders at 3405 and 3425 cm^{-1}).

Indeed, the experiments illustrated in Fig. 3 (concerning the interaction of NH_3 with hydroxylated surfaces) demonstrate well that ammonia interacts with OH groups following the schemes

$$NH_3 + OH^- \rightarrow OH^- \ldots NH_3$$
$$NH_3 + OH^- \rightarrow H_2NH \ldots OH^-. \quad (2)$$

In fact the broad peaks at 3580 and 3050 cm^{-1} can be assigned to $OH^- \ldots N$ and $NH \ldots OH$ stretching modes, respectively, for the following reasons:

(i) with respect to the unperturbed OH and NH groups, the shifts caused by hydrogen bonding are ~200 and ~300 cm^{-1}, respectively (as expected for the formation of hydrogen bonding of weak-medium strength (*13*));

(ii) the half-width of the 3580- and 3050-cm^{-1} peaks (~300 cm^{-1}) is also typical for $OH \ldots N$ and $NH \ldots O$ hydrogen bonds of weak-medium intensity (*13*);

(iii) both frequencies and shifts find precedents in the literature concerning $OH \ldots N$ and $NH \ldots O$ hydrogen bonding (*13*).

As reported in the literature, $NH \ldots N$ hydrogen bonding can also occur (*13*). Consequently the NH_2^- groups formed in the initial dissociation step are expected to interact with NH_3 following the scheme

$$NH_2^- + NH_3 \rightarrow HNH^- \ldots NH_3 \quad (3)$$

and to give $NH \ldots N$ groups absorbing roughly in the same region as the $NH \ldots OH^-$ groups (~3050 cm^{-1}).

The Structure of Adsorbed Oxygen

The structure of adsorbed oxygen has already been discussed in Ref. (*8*). For the sake of clarity we recall that reversible O_2^- (superoxo) species are formed on the surface of solid solutions following the scheme:

$$Co^{2+} + O_2 \rightleftarrows Co^{3+}O_2^-. \quad (4)$$

The stretching frequency of the superoxo species occurs in the range 1250–1000 cm^{-1}, the exact figure being dependent upon the location of the Co^{2+} ions on the MgO surface.

O_2^- species located on the matrix have also been detected by ESR (*10*). Finally, evidence of dissociative chemisorption of O_2 has also been obtained by reflectance spectroscopy (*12*).

The Interaction of NH_3 and O_2 in the Adsorbed State

By interaction of O_2 with adsorbed NH_3 (or by adsorption of NH_3/O_2 mixtures) the following effects are observed:

(i) formation of N_xO_y species (characterized by stretching frequencies in the range 1450–1000 cm^{-1}) (Table 1);

(ii) disappearance of the IR manifestations of the NH_2^- groups;

(iii) extensive formation of hydroxyl groups;

(iv) deep modification of the bands associated with molecularly adsorbed NH_3.

If the same experiment is carried out on the pure matrix a similar, but much slower, process occurs, leading to the destruction of the NH_2^- species and to the formation of reduced quantities of hydroxyls and of oxidized species.

A comparison between the two experiments clearly reveals the role of Co^{2+} ions in favoring the surface oxidation of NH_3. As will be demonstrated in the next paragraph, the oxidized species are mainly represented by NO_2^- and NO_3^- (i.e., $x = 1$ and $y = 2$ or 3).

Plausible reaction schemes for NH_2^- consumption are consequently

$$2NH_2^- + 3Co^{3+}O_2^- + 2O^{2-} \rightarrow 2NO_2^- + 4OH^- + 3Co^{2+} \quad (5)$$

$$NH_2^- + 2Co^{3+}O_2^- + O^{2-} \rightarrow NO_3^- + 2OH^- + 2Co^{2+}, \quad (6)$$

where NO_2^- and NO_3^- are formed in reactions (5) and (6), respectively.

As far as the reaction with molecularly

TABLE 1

Frequencies of IR Absorption Bands and Assignments

Experimental frequency (cm^{-1})	Assignment	$\Delta\bar{\nu}$ (cm^{-1})	
		Experimental	From NO_2^- and NO_3^- in matrix (*10*)
$^{14}N_x{}^{16}O_y$ 1435	$^{14}N^{16}O_3^-(\nu_{3a})$		
1319	$^{14}N^{16}O_2^-(\nu_{as})$; $^{14}N^{16}O_3^-(\nu_{3b})$		
1226	$^{14}N^{16}O_2^-(\nu_s)$		
1048	$^{14}N^{16}O_3^-(\nu_1)$		
$^{15}N_x{}^{16}O_y$ 1399	$^{15}N^{16}O_3^-(\nu_{3a})$	28.5	30.9
1298	$^{15}N^{16}O_2^-(\nu_{as})$; $^{15}N^{16}O_3^-(\nu_{3b})$	21	22
1204	$^{15}N^{16}O_2^-(\nu_s)$	22	25.5
1048	$^{15}N^{16}O_3^-(\nu_1)$	0	0.3
$^{14}N_x{}^{18}O_y$ 1421	$^{14}N^{18}O_3^-(\nu_{3a})$	23.5	19.8
1286	$^{14}N^{18}O_2^-(\nu_{as})$; $^{14}N^{18}O_3^-(\nu_{as})$	33	34.1
1201	$^{14}N^{18}O_2^-(\nu_s)$	25	26.2
987	$^{14}N^{18}O_3^-(\nu_1)$	61	60.4

adsorbed NH_3 is concerned, the following reaction schemes are hypothesized:

$$2NH_3 + 3Co^{3+}O_2^- + 4O^{2-} \rightarrow 2NO_2^- + 6OH^- + 3Co^{2+} \quad (7)$$

$$2NH_3 + 4Co^{3+}O_2^- + 4O^{2-} \rightarrow 2NO_3^- + 6OH^- + 4Co^{2+}. \quad (8)$$

It is most noticeable that in reactions (5)–(8), the Co^{2+} ions act as an oxygen activator through the formation of $Co^{3+}O_2^-$ adducts.

Schemes (5)–(8) explain:

(i) the formation of NO_2^- and NO_3^- species;

(ii) the abundant formation of OH^- groups covering a large fraction of the surface;

(iii) the disappearance of the IR manifestations of NH_3 weakly adsorbed on cations (because after NH_3–O_2 interaction, the surface is largely covered by hydroxyl groups);

(iv) the growth of the IR manifestations of NH_3 adsorbed on OH^- groups (peak at ~3400 cm^{-1}) and of the OH and NH groups perturbed by hydrogen bonding (peaks at 3580 and 3050 cm^{-1}).

Of course, if ND_3 is used instead of NH_3, OD^- and hydrogen-bonded ND_3 are formed, in agreement with the results of Fig. 4.

The Structure of the $N_xO_y^-$ Species

The structure is elucidated by comparing the IR spectra of the interaction products between $^{14}NH_3$ and $^{16}O_2$, between $^{15}NH_3$ and $^{16}O_2$, and between $^{14}NH_3$ and $^{18}O_2$ (Fig. 5).

The following procedure has been adopted for the assignment:

(a) First, we started with the hypothesis that the four bands observed in the range 1450–1000 cm^{-1} for the $^{14}NH_3$–$^{16}O_2$ mixture (and not involving hydrogen atoms) are associated with the stretching modes of surface $^{14}N^{16}O_2^-$ and $^{14}N^{16}O_3^-$ species (Table 1). In the range 1450–1000 cm^{-1} the NO_2^- and NO_3^- groups are expected to show a total number of two (ν_{as} and ν_s) and three (ν_{3a}, ν_{3b}, and ν_a) modes, respectively (*14, 16*). Consequently, a mixture of NO_2^- and NO_3^- should show five bands. The observation of only four bands is due to the coincidence of ν_s (NO_2^-) and ν_{3b} (NO_3^-) species.

(b) Second, we compared the spectra obtained by $^{15}NH_3$–$^{16}O_2$ and $^{14}NH_3$–$^{18}O_2$ interaction with those of $^{15}N^{16}O_2^-$, $^{15}N^{16}O_3^-$,

$^{14}N^{18}O_2^-$, and $^{14}N^{18}O_3^-$ in KBr matrix (in particular the isotopic shifts with respect to the unmarked compounds are compared in Table 1).

(c) The similarity between the experimental shifts and those of NO_2^- and NO_3^- trapped species (*17*) is very satisfactory. Consequently (and finally) we considered this result as a proof of the initial tentative assignment.

Further proofs of this assignment can be derived from the experiments illustrated in Figs. 6 and 7.

The first experiment demonstrates that the 1204-cm^{-1} peak corresponds to an oxidizable species (in agreement with the hypothesized NO_2^- structure) while the peaks at 1430–1400, 1300–1270, and 1048 cm^{-1} correspond to a fully oxidized species (in agreement with the hypothesized NO_3^- structure) because their intensity increases upon oxidation.

The second experiment shows that the 1399- and 1298-cm^{-1} peaks assigned to the stretching modes of the NO_3^- species move with the quantity of coadsorbed NH_3 in the way expected for the equilibrium

$$\underset{\text{“contact pair”}}{Me^{2+}NO_3^-} \ \underset{-NH_3}{\overset{+NH_3}{\rightleftarrows}} \ \underset{\text{“solvent-separated pair”}}{Me^{2+}\|NO_3^-}$$

In fact, in homogeneous conditions, the frequency separation of the NO_3^- modes of "contact pairs" is larger than that of "solvent-separated pairs" (for NO_3^- ions in real D_{3h} symmetry only one peak is expected corresponding to a doubly degenerate mode) (*14, 16*). The close behavior of the vibrational properties of the NO_3^- ion on the surface and in solution proves definitely that the bands at 1399 and 1298 cm^{-1} belong to the NO_3^- species: consequently the whole group of hypotheses concerning the oxidized species receives further support.

The presence of nitrites among the partially oxidized species indicates that at room temperature the oxidation process is not complete.

This consideration suggests that also less oxidized species (for instance, NO^-) should perhaps be taken into account. The frequency of NO^- in negatively charged nitrosylic compounds is normally in the range 1700–1500 cm^{-1} (*14*). The NO^- frequency in Li^+NO^- trapped in a cryogenic matrix has been observed at 1353 cm^{-1} (*18*). A species absorbing at 1068 cm^{-1} has also been found when NO is adsorbed on alkali halides (*19*) and has been assigned to a NO^- structure.

Following these literature data we expect that a hypothetical NO^- species should give a single peak in the broad interval 1700–1000 cm^{-1}. The IR spectrum in the range 1700–1000 cm^{-1} does not clearly show the presence of such a single uncoupled band: consequently the NO^-, if present, cannot be seen easily by IR (because its IR manifestations are obscured by those of the NO_2^- and NO_3^-).

CONCLUSIONS

Cobalt ions emerging at the surface of MgO–CoO solid solutions promote the room temperature oxidation of NH_3 with formation of NO_2^- and NO_3^- species. As species in lower oxidation state were not detected, we conclude that O_2^- is a highly active oxidizing species.

The vibrational assignment of the interaction products is given by comparing the IR spectra of $^{14}NH_3$–$^{16}O_2$, $^{14}ND_3$–$^{16}O_2$, $^{15}NH_3$–$^{16}O_2$, and $^{14}NH_3$–$^{18}O_2$ interaction products.

ACKNOWLEDGMENT

This work was supported by the Ministero della Pubblica Istruzione, Progetti di Rilevante Interesse Nazionale.

REFERENCES

1. Gland, J. L., and Karchak, V. N., *J. Catal.* **53,** 9 (1978).
2. Gland, J. L., and Woodard, G. C., and Karchak, V. N., *J. Catal.* **61,** 543 (1980).

3. Flytzani-Stephanapoulos, M., Shmidt, L. S., and Carretta, R., *J. Catal.* **64,** 346 (1980).
4. Il'chenko, N. I., and Godolets, G. I., *J. Catal.* **39,** 57 (1975).
5. Morikawa, S., Takahashi, K., Hoshida, H., and Kurita, S., *in* "Proceedings, 8th Int. Cong. on Catalysis, Berlin, 1984, Vol. III, p. 661. Dechema, Frankfurt, 1984.
6. Griffiths, D. W. L., Hallam, H. E., and Thomas, W. J., *J. Catal.* **17,** 18 (1970).
7. Zecchina, A., and Spoto, G., *J. Catal.* **96,** 586 (1985).
8. Zecchina, A., Spoto, G., and Coluccia, S., *J. Mol. Catal.* **14,** 351 (1982).
9. Coluccia, S., Garrone, E., and Borello, E., *J. Chem. Soc., Faraday Trans. 1* **79,** 607 (1983).
10. Cordischi, D., Indovina, V., Occhiuzzi, M., and Arieti, A., *J. Chem. Soc., Faraday Trans. 1* **75,** 533 (1979).
11. Jones, D. R., Summerville, D. A., and Basolo, F., *Chem. Rev.* **79,** 139 (1979).
12. Hagan, A. P., Lofthouse, M. G., Stone, F. S., and Trevethan, M. A., *in* "Scientific Basis for the Preparation of Heterogeneous Catalysts" (B. Delmon, P. Grange, P. Jacoband, and G.Poncelet, Eds.), p. 417. Elsevier, Amsterdam, 1972.
13. Pimentel, G. C., and McClellan, A. L., *in* "The Hydrogen Bond" (L. Pauling, Ed.), Chap. 3, p. 67. Reinhold, New York, 1960.
14. Nakamoto, K., "Infrared Spectra of Inorganic and Coordination Compounds." Wiley, New York, 1970.
15. Coluccia, S., Lavagnino, S., and Marchese, L., *J. Chem. Soc. Faraday Trans. 1,* in press.
16. Devlin, J. P., and Consani, K., *J. Phys. Chem.* **88,** 3269 (1984).
17. Kato, R., and Rolfe, J., *J. Chem. Phys.,* **47,** 1901 (1967).
18. Laane, J., and Ohlsen, J. R., *Prog. Inorg. Chem.* **27,** 465 (1980).
19. Smart, R. St. C., *Trans. Faraday Soc.* **67,** 1183 (1971).